The 2018 World Congress on
Advances in Civil, Environmental, & Materials Research (ACEM18)
Songdo Convensia, Incheon, Korea, August 27 - 31, 2018

Direct shear simulation of geosynthetic-reinforced specimen using 3D-DEM

*Hoang-Khanh Le[1)], Wen-Chao Huang[2)] and Chih-Chun Chien [3)]

[1), 2), 3)] *Department of Civil Engineering, National Central University, Taoyuan City, 32001, Taiwan*
[1)] *lehoangkhanhhaugiang@gmail.com*

ABSTRACT

Geosynthetic material is widely used for stabilizing weak or loose material in geotechnical engineering. For example, the possible excessive rut depths of roadways may be reduced by including geogrid and geotextile between the base and subgrade layers. In this study, a series of Direct Shear (DS) tests with and without geogrid at the interface of base and subgrade layers were simulated using 3D-Discrete Element Method (3D-DEM) to explore the shear stress at various shear displacements, especially under large shear displacements. First of all, the DEM models were verified by comparing them with the experimental results by Liu, et al. (2009). Similar results were observed that the shear strength of the simulated geogrid-reinforced cases was smaller than that of unreinforced cases under small shear displacement. However, in the simulation, the shear strength of the reinforced model was doubled comparing to that of the unreinforced case under large shear displacement. The results may indicate that the shear strength obtained in the literature was not fully mobilized yet. On the other hand, the shear strength of the geogrid-reinforced specimen under direct shear condition could only be activated under large displacements. Finally, the effect of different aperture sizes were also simulated with DS simulation. It was found that the aperture size may have an optimum reinforcing effect with respect to the particle size.

[1)] Ph.D. Student
[2)] Associate Professor
[3)] Ph.D. Student

1. INTRODUCTION

Strength and stiffness of a subgrade foundation play an important role on the long-term performance of roadways, especially for unpaved ones. With development of economy, requirement of roadway construction on week subgrade with low shear strength such as clay and silt soils is unavoidable. Some soil stabilization approaches comprising cement-treated technique, compaction, and excavation-replacement have been used in the past few years. However, these methods somehow show high cost, time-consuming and low efficiency, especially for weak soils with relatively high ground water table. An alternative effective method, which is widely used in recent years, is geogrid reinforcement. Geogrid shows a significant contribution in enhancing the bearing capacity of the system, which helps decrease shear stresses on the subgrade soil.

The contribution of geogrid reinforcement to the interface shear strength of soil-geogrid system has been investigated using direct shear test by many researchers (Alfaro et al. 1995; Bakeer et al. 1998.). Jewell et al. (1984) pointed out the important reinforcing mechanism of interlocking between the geogrid and aggregate particles in reinforced pavement systems. Alfaro et al. (1995) and Tatlisoz et al. (1998) demonstrated that the shear strength of the soil-geogrid interface came from two components including (1) the shear resistance between soil and the ribs and (2) the internal shear resistance of the soil in the opening area. Lee at el. (2012) also reported that the peak shear strength of the soil-geogrid-aggregate in large scale direct shear tests strongly depended on the geogrid type, subgrade and aggregate properties and test conditions; two critical factors such as aperture area and junction strength directly influenced the overall interface shear strength. Tutumluer et al. (2012) used the aggregate image aided DEM model to evaluate the interlock mechanism of geogrid-aggregate. The results showed that the geogrid geometries such as rectangular and triangular shaped apertures strongly affected the stiffness of reinforced system and resulted in better mobilized shear resistance along the shear plane. Liu et al. (2009) conducted some large scale direct shear tests to evaluate the passive resistance contribution of geogrid to the overall shear strength of sand-geogrid interfaces. The results showed that the shear stress of the sand-geogrid interface was smaller than that of sand-sand interface at relatively small shear displacement (Fig. 1). However, the interface shear stress of the sand-geogrid model, which continued increasing, was unknown because of the limitation of laboratory apparatus in applying shear displacement. The main objective of this study is to investigate the contribution of geogrid to the interface shear strength of particle-geogrid at large shear displacement. To achieve this target, a series of direct shear tests with various aperture sizes of geogrid were simulated using 3D-DEM. Then, fundamental characteristics of geogrid such as aperture size and interlocking behavior, which influence the overall shear stress of particle-geogrid, are discussed.

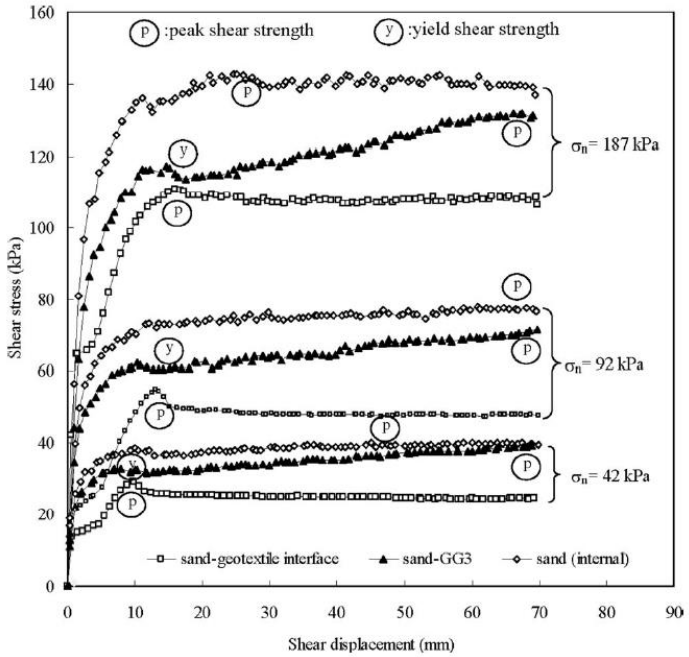

Fig. 1 Shear stress v.s. shear displacement of reinforced and unreinforced samples in direct shear test (Liu et al., 2009).

2. NUMERICAL TESTING PROCEDURE

In this study, direct shear test with a layer of geogrid at the predetermined shear plane was simulated using three-dimensional discrete element method (3D-DEM). Firstly, geogrid layer with a given aperture size was generated by a connection of some particles at the designed positions. All particles of the simulated geogrid layer were connected using parallel bonding with given tensile strength which must be reasonably large to avoid the broken of the geogrid during shearing. The particles of geogrid layer along the boundary were fixed to prevent the geogrid from moving during shearing. In this investigation, three different aperture sizes of geogrid layer with square shape which are 20 mmx20 mm, 24 mmx24 mm and 28 mmx28 mm were simulated (Fig. 2). Afterward, assembly of particles with a uniform radius of 2.5mm and a given porosity was generated in the upper and lower parts of the direct shear box. The length, the width and the height of the shear sample were 100mm, 100mm and 60mm, respectively (Fig. 3). The micro-parameters of particles and geogrid layer in the DEM models were shown in Tab. 1.

The lower part of the DEM model contained 5 walls which can move horizontally at a constant speed of 1 mm/s to the right during the test. Four walls (No. 11, 12, 13 and 14) were constructed at the upper part of specimen as stationary boundaries. Especially, the top wall of the upper part of box could move freely in the vertical direction to adjust its pressure corresponding to the normal stresses of 50, 100 and 150kPa, which was always remained constant during the shear time. In addition, two walls were also added at the center of the sample to avoid any movement of the particles going out of the model during

the simulated process. The simulations were stopped when the total shear displacement reached approximately 16 mm, which corresponded to 16% of the shear specimen width (i.e. 100 mm). Reaction forces between wall 12 and wall 14 (or between wall 8 and wall 10) was recorded to estimate the shear force through the center of specimen during the shearing process (Fig. 4). Then the shear stress was calculated with the shear force (Eqs. 1 and 2) dividing the horizontal cross section area. In this study, the force acting on other walls was not considered except the top wall because their reaction force were so small and can be neglected.

$$F\ (force) + R_{12}(reaction\ force\ on\ wall\ 12) = R_{14}(reaction\ force\ on\ wall\ 14) \quad (1)$$

$$F\ (force) + R_{10}(reaction\ force\ on\ wall\ 10) = R_{8}(reaction\ force\ on\ wall\ 8) \quad (2)$$

Tab. 1 The micro-parameters of particles and geogrid in DEM models

Property	Geogrid	Particle
Effective modulus (Pa)	$3.6x10^9$	10^8
Normal to shear stiffness ratio (-)	1	2.5
Friction coefficient (-)	-	1.1
Tensile strength (Pa)	$1.5x10^{12}$	-
Cohesion (Pa)	$1.5x10^{12}$	-
Friction angle (degrees)	0	-

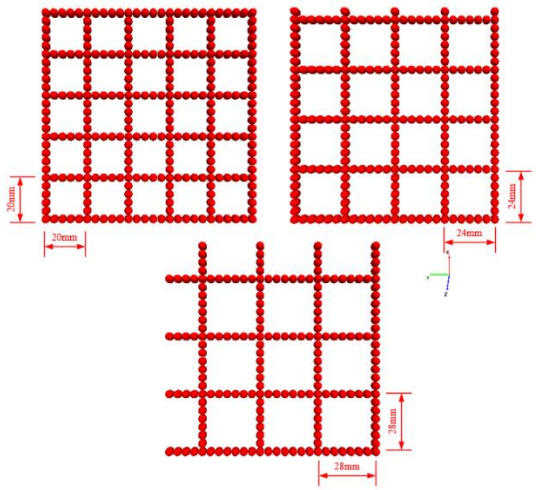

Fig. 2 Simulation of geogrid layer with the given aperture sizes at 20mm, 24mm and 28mm.

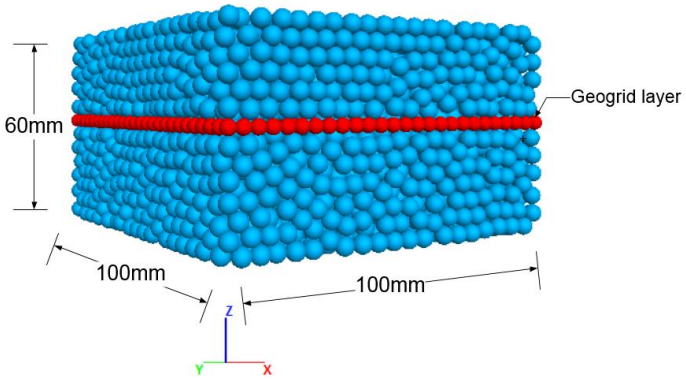

Fig. 3 Dimensions of direct shear sample in the DEM model.

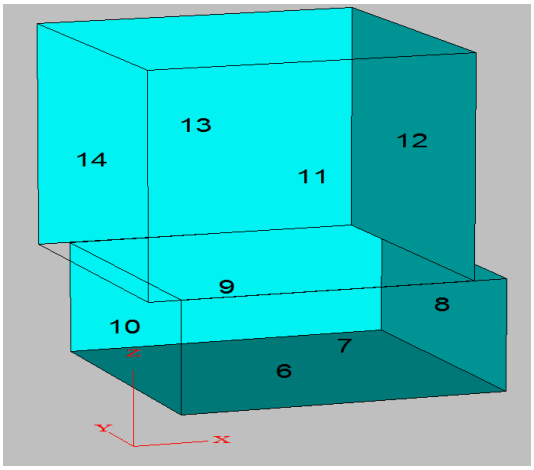

Fig. 4 Illustration of the walls in three-dimensional DEM model

3. SIMULATION RESULTS

Figure 5 showed the DS test results for unreinforced and reinforced geogrid models. The peak strength of unreinforced model was almost obtained at the shear displacement of 1mm and reduced to a residual strength until the end of the test; the peak shear stresses under different normal stresses of 50, 100 and 150kPa were 20, 37 and 52kPa, respectively. Under small shear displacement (less than 6mm), the shear stress of all models with geogrid reinforcement was smaller than that without geogrid reinforcement, which was similar to what was observed by Liu et al. (2009). However, the shear stress of reinforced models continued to increase at larger shear displacement up to 16mm. The increase of shear stress in reinforced cases may be due to the contribution of geogrid with interlocking mechanism along the shear plane. After some initial shear displacements, particles within aperture of geogrid were rearranged and interlocked as shown in Fig. 6, in which the cross sections shown were 5mm below and above the geogrid. Figure 7 illustrated the distribution of contact forces at the geogrid layer before and after the test; negative contact force indicated tension. The result clearly showed that most of contact forces in the geogrid layer were tensile force which contributed to interlock particles within

the aperture of geogrid and to reduce vertical deformation of particle assembly during shearing. Figure 8 showed the simulation results in friction angles of different models with and without geogrid reinforcement. The results indicated that all of reinforced models with geogrid at the interface yielded higher friction angles than the model without geogrid. Especially, the friction angle of the model with geogrid aperture size of 24 mmx24 mm was the greatest in the group (24 degrees) while the friction angle of the model without geogrid was 18 degrees. It could be concluded that geogrid with various aperture sizes may have different influences to the overall shear strength of the reinforced models. It seems that the models reinforced with geogrid may also contribute to the increase of cohesion for the overall system.

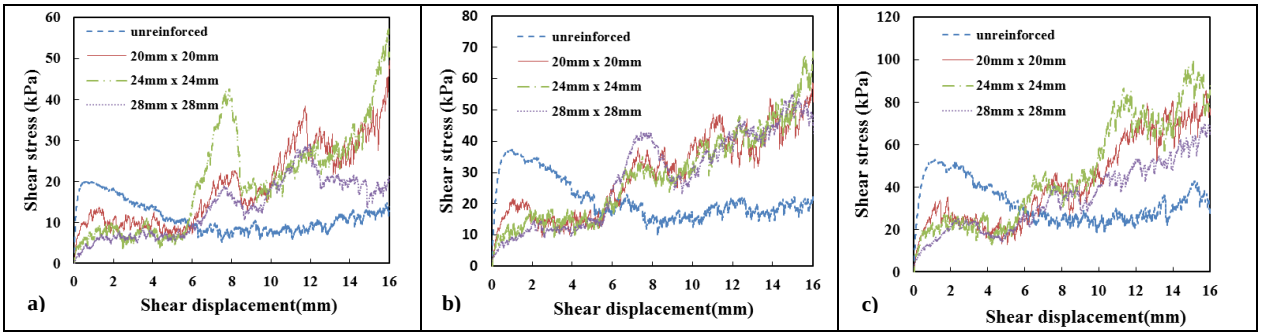

Fig. 5 Shear stress v.s. shear displacement for unreinforced and reinforced models under various normal stresses: a) Normal stress of 50 kPa; b) Normal stress of 100 kPa; c) Normal stress of 150 kPa.

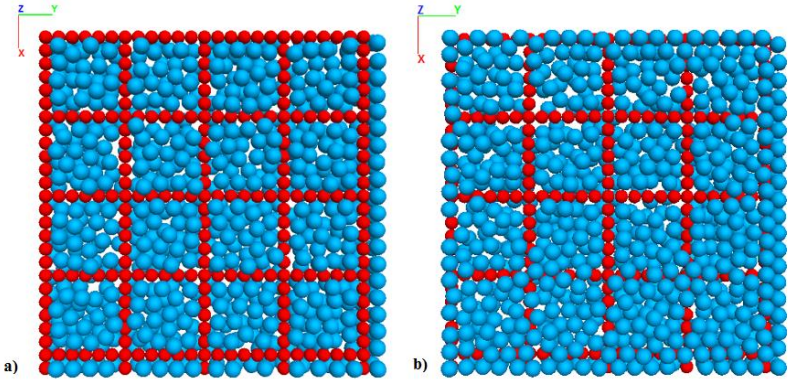

Fig. 6 Interlocking of particles within aperture of geogrid (24mm x 24mm) under normal stress of 100kPa: a) before shearing; b) after shearing.

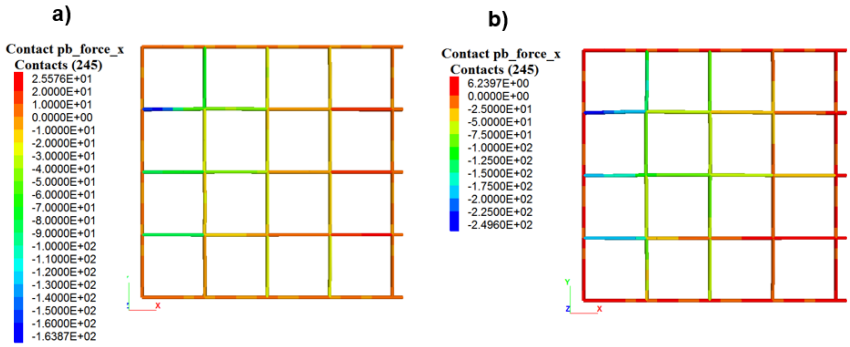

Fig. 7 Distribution of tensile forces (negative values) at the geogrid layer under normal stress of 100kPa: a) before the test (maximum tensile force is 164N); b) after the test (maximum tensile force is 250N).

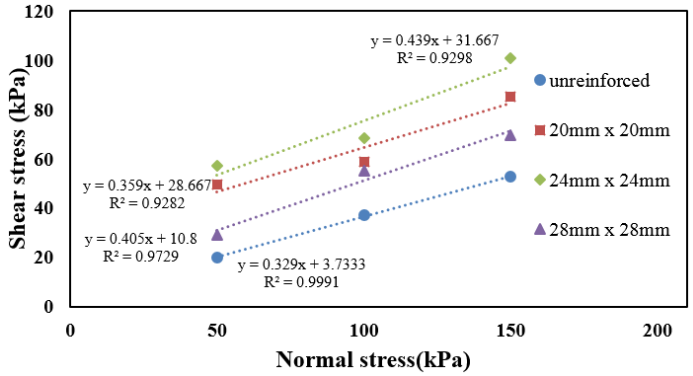

Fig. 8 Analysis results in friction angle for unreinforced and reinforced models.

Dilation behavior of models with and without geogrids under different normal stresses was shown in Fig. 9. The vertical displacement of these models was approximately 2.5mm at the end of the test. For reinforced model with geogrid, the change in the height of sample was less than 0.5mm, which indicated that geogrid layer helped reduce the vertical displacement of particles during shearing. Model with geogrid aperture size of 24 mmx24 mm almost showed contraction behavior, which demonstrated that the most effective aperture size of geogrid may help to rearrange and interlock particles in the best way.

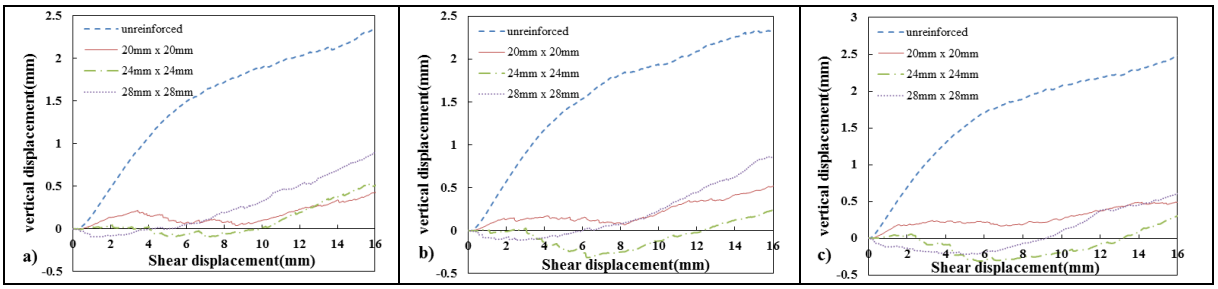

Fig. 9 Dilation and contraction behavior of unreinforced and reinforced models under different normal stresses: a) Normal stress of 50 kPa; b) Normal stress of 100 kPa; c) Normal stress of 150 kPa.

Figure 10 illustrated the simulation results of the direct shear tests to estimate the effect of the aperture area of geogrid on the peak shear strength of models simulated with and without geogrid in place. In this study, the average interface shear strength coefficient of α, which was usually used to evaluate the effectiveness of geogrids, was defined as the ratio of the shear strength of model with geogrid reinforcement to the shear strength of model without the geogrid reinforcement, both measured under the same normal stress. The value of α ranging from 1.3 to 2.9 was recorded. The test results clearly indicated that the geogrid with the aperture size of 24 mmx24 mm produced the highest average peak interface shear strength. The optimum aperture area of the geogrid was 576mm^2, which was considered in this investigation. As a result, the effective ratio of the aperture size (24mm) and the diameter of particle (5mm) using in this study could be calculated as 4.8.

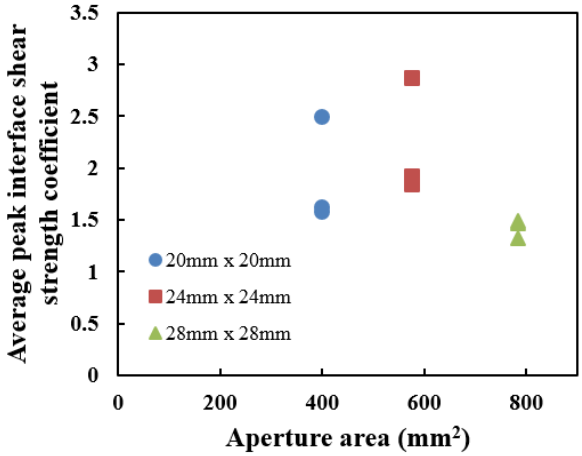

Fig. 10 Effect of the geogrid aperture area on the average peak interface shear strength coefficient.

4. CONCLUSIONS

A series of direct shear tests with and without geogrid reinforcement were simulated to investigate effectiveness of geogrid to the overall shear strength of material. All of

reinforced models were tested with various aperture sizes of 20mmx20mm, 24mmx24mm and 28mmx28mm. The highlight of this investigation can be summarized as follow:

a) Geogrid reinforcement plays an important role on increasing the peak shear strength of material along the shear plane. The peak shear strength of model with geogrid at the interface may increase as doubled even tripled compared to that of model without geogrid under large shear displacements. This may be attributed to the effect of particles interlocking within the aperture of geogrid.

b) The friction angle of models with geogrid reinforcement was almost higher than that without geogrid reinforcement. The geogrid layer helps to reduce the vertical displacement of particles assembly during shearing.

c) In this study, the average interface shear strength coefficient α was used to estimate the effect of the geogrid aperture to the average peak interface shear strength of direct shear model. The value of α is ranged from 1.3 to 2.9. The optimum aperture area of geogrid was observed as 576mm^2 in this investigation.

This study only focuses on numerical simulation using DEM. Therefore, some laboratory tests may need to be conducted and compared with the results obtained in this investigation.

REFERENCES

Alfaro, M., N. Miura, and D. Bergado, Soil-Geogrid Reinforcement Interaction by Pullout and Direct Shear Tests. 1995.

Bakeer, R.M., et al., Pullout and shear tests on geogrid reinforced lightweight aggregate. Geotextiles and Geomembranes, 1998. 16(2): p. 119-133.

Jewell, R.A., G.W.E. Milligan, and D. Dubois, Interaction between soil and geogrids, in POLYMER GRID REINFORCEMENT. p. 18-30.

Liu, C.-N., et al., Behavior of Geogrid-Sand Interface in Direct Shear Mode. Journal of Geotechnical and Geoenvironmental Engineering, 2009. 135(12): p. 1863-1871.

Tatlisoz, N., B. Edil Tuncer, and H. Benson Craig, Interaction between Reinforcing Geosynthetics and Soil-Tire Chip Mixtures. Journal of Geotechnical and Geoenvironmental Engineering, 1998. 124(11): p. 1109-1119.

Tutumluer, E., H. Huang, and X. Bian, Geogrid-Aggregate Interlock Mechanism Investigated through Aggregate Imaging-Based Discrete Element Modeling Approach. International Journal of Geomechanics, 2012. 12(4): p. 391-398.

Lee, M. S., Y. S. Choi, and M. Prezzi Quality Assessment of Geogrids Used for Subgrade Treatment. Publication FHWA/IN/JTRP-2012/27. Joint Transportation Research Program, Indiana Department of Transportation and Purdue University, West Lafayette, Indiana, 2012. doi: 10.5703/1288284315034.